Topological Analysis of the Electron Density Distribution in the Crystal of 8,9,10,12-Tetrafluoro-*o*-carborane on the Basis of the High-Resolution X-ray Diffraction Data at 120 K

Konstantin A. Lyssenko, Mikhail Yu. Antipin,* and Viatcheslav N. Lebedev

Institute of Organoelement Compounds (INEOS), Russian Academy of Sciences, Vavilov Street 28, B-334, Moscow 117813, Russia

Received July 7, 1998

A topological analysis of the electron density distribution $\rho(\mathbf{r})$ in the crystal of 8,9,10,12-tetrafluoro-*o*-carborane $C_2B_{10}H_8F_4$ was performed using high-resolution low-temperature (120 K) X-ray diffraction data (14 606 reflections, $R = 0.026$) and a multipole model for data refinement. Molecules in the crystal (space group *Pbcn*, $Z = 4$) occupy special positions on a 2-fold symmetry axis passing through the middle of a C−C bond and the opposite B−B bond of the octahedral cage. Deformation electron density maps as well as maps of the Laplacian of $\rho(\mathbf{r})$ showed that electron density is essentially delocalized over the surface of the cage and locally depleted in its center. All B−B and B−C bonds in the polyhedron are characterized by significant bending, which is evident in shifts of their (3,−1) bond critical points from the straight lines between bonded atoms. Detailed analysis of $\rho(\mathbf{r})$ values and its Laplacian in the bond critical points revealed some unexpected features in the bonding pattern of the structure studied, namely, the positive value of the Laplacian in the homopolar C−C bond and the negative values for the B−C bonds. These data are compared with corresponding ab initio calculations of small deltahedral boranes and carboranes. It is concluded that the electron-withdrawing effect of the fluorine atoms causes considerable redistribution of the electron density in the molecule, and, in particular, this is reflected in the shift of $\rho(\mathbf{r})$ from the more electron-rich C−C bonds to the B−C bonds.

Introduction

The nature of the chemical bond in the polyhedral *closo*-borane dianions $B_nH_{2n}^{2-}$ and isoelectronic *closo*-carboranes $C_2B_{n-2}H_n$ (with the *n* value varying in the interval $5 \le n \le 12$) has a great interest because of the electron-deficient and multicenter character of these molecules. The bonding pattern in this class of molecules was one of the first examples in which the common chemical language of the Lewis electron pair model could not sufficiently describe the bonds.

In early years, Liscomb's Styx formalism,[1] Wade's rules,[2,3] and William's classification of the *closo*-boranes and carboranes[4] were the most widely used concepts and electron counting schemes for prediction the molecular structures, properties, and relative stability of the different closed cages and their possible isomers. Later, more sophisticated models for description of the structure of the *nido*- and *closo*-boranes and carboranes, such as tensor surface harmonics by Stone,[5,6] the "six-electron rule" by Jemmis,[7] and the graph-theoretical analysis and three-dimensional aromaticity by King,[8,9] led to a much more serious understanding the nature of the chemical bonding in these deltahedral molecules. We should note that all of these models dealt only with the molecular-orbital (and/or energetic) description of the structures of boranes and carboranes.

On the other hand, very attractive description and distinct interpretation of the chemical bonds in these electron-deficient molecules are also possible on the basis of the electron density (or charge density) distribution analysis. The electron density distribution (EDD) function $\rho(\mathbf{r})$ of a molecular system defines many of its properties, including, as well, the pattern of the chemical bonding (see, for example[10−12]). Direct information about the nature of the chemical bond may be obtained via analysis of the $\rho(\mathbf{r})$ function in terms of its topological characteristics (gradient vector field, Laplacian of $\rho(\mathbf{r})$, types and position of the critical points of $\rho(\mathbf{r})$, bond paths, etc.) following Bader's theory of atoms in molecules[10,11] or in terms of features of the deformation (difference) electron density $\delta\rho(\mathbf{r})$, i.e., the difference between the total electron density $\rho(\mathbf{r})$ and electron density of the specially defined "reference" state.[13]

The attractiveness of this approach in the modern analysis of the chemical bond is caused by two reasons. First, the EDD function is an observable value, it has clear physical meaning, and allows one a simple visualization in the electron density maps or maps of some of its characteristics, such as Laplacian or $\delta\rho(\mathbf{r})$. On the other hand, the $\rho(\mathbf{r})$ function as well as its topological characteristics and $\delta\rho(\mathbf{r})$ may now be reconstructed

(1) Liscomb, W. N. *Boron Hydrides*; Benjamin: New York, 1963.
(2) Wade, K. *J. Chem. Soc., Chem. Commun.* **1971**, 792−793.
(3) Wade, K. *Adv. Inorg. Radiochem.* **1976**, *18*, 1−66.
(4) Williams, R. E. *Chem. Rev.* **1992**, *92*, 177−207.
(5) Stone, A. J. *Mol. Phys.* **1980**, *41*, 1339−1354.
(6) Stone, A. J. *Inorg. Chem.* **1981**, *20*, 563−571.
(7) Jemmis, E. D. *J. Am. Chem. Soc.* **1982**, *104*, 7017−7020.
(8) King, R. P.; Rouvray, D. H. *J. Am. Chem. Soc.* **1977**, *99*, 7834−7840.
(9) King, R. P.; Dai, B.; Gimarc, B. M. *Inorg. Chim. Acta* **1990**, *167*, 213−222.
(10) Bader, R. F. W. *Atoms in Molecules: A Quantum Theory*; Oxford University Press: Oxford, U.K., 1990; 438 pp.
(11) Kraka, E.; Cremer, D. In *Theoretical Models of Chemical Bonding, Part 2, The Concept of the Chemical Bond*; Maksic, Z. B., Ed.; Springer-Verlag: Berlin, 1990; pp 453−487.
(12) Tsirel'son, V. G.; Ozerov, R. P. *Electron Density and Bonding in Crystals*; IOP Publ.: London, U.K., 1996; 517 pp.
(13) Coppens, P. *Annu. Rev. Phys. Chem.* **1992**, *43*, 663−692.

10.1021/ic9807644 CCC: $15.00
Published on Web 10/15/1998

with high accuracy from the single-crystal X-ray diffraction data.[12−14] Therefore this approach allows one to describe the nature of the chemical bonds in molecules and crystals on the basis of measured (observable) quantities.

Nevertheless, similar analysis of the charge density distribution in the *closo*-borane and *closo*-carborane molecules (calculated theoretically or reconstructed from the X-ray diffraction data) has been performed only for a small number of such compounds, and there are only a few recent papers in the literature[15,17−21] where an electronic structure of these molecules was analyzed in terms of the EDD characteristics.

Takano et al.[15] used an analytical approach ("spherical charge analysis") by Iwata[16] for analysis of the electron-deficient three-center two-electron bonds in $B_nH_n^{2-}$ and $C_2B_{n-2}H_n$ ($5 \leq n \leq 12$) cages with deltahedral skeletons. Deformation electron density (DED) maps based on the ab initio RHF calculations with the STO-6G and MIDI-4 basis sets were constructed for dianions $B_5H_5^{2-}$, $B_6H_6^{2-}$, and $B_7H_7^{2-}$. In accord with calculations, external B−H bonds in dianions have a homopolar two-electron two-center nature, central rings have a charge distribution similar to that for planar conjugated systems, and central parts of the cages are electronically empty. The extra (2−) charge is delocalized over the surface of the cages.

More detailed theoretical investigation of the chemical bonding and reactivity in the large series of simplest boranes and *closo*-carboranes was made by Bader and Legare[17] in terms of Bader's topological theory of atoms in molecules (AIM).[10] According to this analysis, stabilization of the electron-deficient molecules is achieved not only by accumulation of the electronic charge along the bond paths but also by its attendant concentration within and its delocalization over the rings of the bonded atoms, which results in the formation of many additional interatomic linkages.

A very similar analysis of the EDD including molecular electrostatic potential calculations for a series of 5−7-vertex *closo*-boranes, carboranes, and silaboranes has been performed by Jemmis et al.[18] In addition to discussion of the EDD topological characteristics and electrostatic potential features in these molecules, some conclusions about the reactivity of the *closo*-deltahedral molecules were made in the cited paper.[18]

Nevertheless, all these results refer only to the theoretically calculated electron density. Experimental studies of the charge density distribution in crystals of boranes and carboranes are very rare.[19−21] This is remarkable considering the great number of papers devoted to the chemistry and quantum-chemical calculations of these molecules, in particular performed for icosahedral *closo*-carboranes. After the first accurate EDD analysis of the crystal structure of decaborane by Dietrich and Scheringer[19] in 1978, only two papers were published later by Antipin et al.[20,21] where an EDD study in the *closo*-carborane derivatives has been performed, namely for electron-deficient icosahedral 9-azido-*m*-carborane[20] and electron-precise pentaethyl-1,5-dicarba-*closo*-pentaborane, $C_2B_3(Et)_5$, representing the smallest carborane cage.[21]

It was found for 9-azido-*m*-carborane that positive DED is distributed continuously over the surface of the icosahedron and it is depleted within the center of the cage. In this paper one of the first topological analysis of the EDD reconstructed directly from the high-resolution X-ray diffraction data was made using a calculation of the Laplacian map via a Fourier series (see ref 22). The modern multipole model for an analytical presentation of $\rho(\mathbf{r})$ function (see for examples refs 13, 14, and 23) was not applied that time, and therefore more detailed study of the topological characteristics of the EDD has not been done for this molecule.

Similar topological analysis has been performed very recently[21] for the trigonal-bipyramidal $C_2B_3(Et)_5$ molecule using high-resolution X-ray diffraction data at 120 K and the XD package program for multipole presentation of $\rho(\mathbf{r})$ and its topological characteristics.[24] It was shown that the bonding pattern in this formally electron-precise molecule may be described as a superposition of the conventional localized two-center bonds between B−C and C−C atoms and multicenter bonding in the triangle B−C−B faces of the C_2B_3 cage. No direct B−B bonds (no bond path in accord with Bader's description) were found in this molecule despite rather short B−B distances (1.876 Å). The center of the cage is characterized by the presence of the (3,+3) critical point, i.e., by the local minimum of the total electron density. This result, especially the absence of the B−B bond path, was found to be in agreement with the theoretical data by Bader and Legare[17] for the simplest carborane molecule $C_2B_3H_5$ having the same deltahedron cage. An essential delocalization of the electron density over the faces of this cage is evident in the relatively high values found for the charge density at the ring critical points compared to the peripheral bond critical points (0.67 and 1.14 e/Å^3, respectively), which might be a characteristic feature of such molecules. It is interesting to note, that in the recent quantum-chemical calculation by Schleyer et al.[25] of the same simplest carborane $C_2B_3H_5$, a conclusion about nonclassical contribution in the bonding pattern in this molecule has received an additional confirmation. In Schleyer's analysis, however, the authors used natural population analysis to characterize the nature of the bonding and results of the energetic and magnetic properties calculations but did not use topological analysis of the charge density that allows one to obtain an answer to the question as to whether two atoms are bonded directly to one another.

On the other hand, in the larger carborane cages, including icosahedral ones, it is reasonable to suggest that the EDD and the bonding pattern may differ from those in small carboranes. Therefore, to provide more experimental information about the electron density distribution and its topological properties in *closo*-carboranes, in the present paper we report the low-temperature (120 K) high-resolution X-ray diffraction analysis of the EDD in the crystal of 8,9,10,12-tetrafluoro-*o*-carborane,

(14) *The Application of Charge Density Research to Chemistry and Drug Design*; Jeffrey, G. A., Piliela, J. F., Eds.; NATO ASI Series B; Plenum Press: New York, 1991; Vol. 250, 409 pp.
(15) Takano, K.; Izuho, M.; Hosoya H. *J. Phys. Chem*. **1992**, *96*, 6962−6969.
(16) Iwata, S. *Chem. Phys. Lett*. **1980**, *69*, 305.
(17) Bader, R. F. W.; Legare, D. A. *Can. J. Chem*. **1992**, *70*, 657−676.
(18) Jemmis, E. D.; Subramanian, G.; Srivastava, I. H.; Gadre, R. *J. Phys. Chem*. **1994**, *98*, 6445−6451.
(19) Dietrich, H.; Scheringer, C. *Acta Crystallogr., Ser. B* **1978**, *34*, 54−63.
(20) Antipin, M. Yu.; Poliakov, A. V.; Tsirel'son, V. G.; Kappham, M.; Grushin, V. V.; Struchkov, Yu. T. *Organomet. Chem. USSR* **1990**, *3*, 421−426.
(21) Antipin, M. Yu.; Boese, R.; Blaeser D.; Maulitz, A. *J. Am. Chem. Soc*. **1997**, *119*, 326−333.
(22) Tsirel'son, V. G. *Canad. J. Chem*. **1996**, *74*, 1171−1179.
(23) Hansen, N. K.; Coppens, P. *Acta Crystallogr., Ser. A* **1978**, *34*, 909−921.
(24) Koritsanszky, T.; Howard, S.; Mallinson, P.; Su, Z.; Richter, T.; Hansen, N. K. *XD: Computer Program Package for Multipole Refinement and Analysis of Electron Densities from Diffraction Data*, Version 1997.
(25) Schleyer, P. v. R.; Subramanian, G.; Dransfeld, A. *J. Am. Chem. Soc*. **1996**, *118*, 9988−9989.

Table 1. Crystal Data and Structure Refinement Results

empirical formula	$C_2H_8B_{10}F_4$
molecular weight, M	216.18
cryst syst	orthorhombic
space group, Z	*Pbcn*, $Z = 4$
radiation	Mo Kα, graphite monochromator
a, Å	6.808(1)
b, Å	11.777(2)
c, Å	11.856(2)
volume, Å^3	950.6(3)
ρ_{calc} (g cm^{-3})	1.511
μ (mm^{-1})	0.126
F(000)	424
T (K)	120(2)
scan type	$\theta/2\theta$ with variable scan speed 2.0−20.0°/min
2θ range (deg)	2.0 to 94.0
no. of reflcns collcd	14606
no. of unique reflcns	4121 ($R_{int} = 0.94\%$)
obsd reflcns	2896 (with $\|F\| > 4.0\sigma(F)$)
weight scheme	$w^{-1} = \sigma^2(F) + 0.0006F^2$
no. of parameters refined	89
goodness-of-fit	1.26
R	0.0334
R_w	0.0352
largest diff peak/hole (e Å^{-3})	0.23/−0.17

$C_2B_{10}H_8F_4$ (**1**). This compound is interesting for such analysis not only as an example of the nonstudied earlier *o*-carborane isomers but also as a representative of the "super" electron-deficient molecule caused by the electron-withdrawing effect of the four neighboring fluorine atoms. The new synthetic route to **1** and its molecular and crystal structure were shortly described earlier in ref 26. An important result of this X-ray study was that the molecules of **1** in the crystal occupy special positions with the 2-fold axis symmetry (space group *Pbcn*, $Z = 4$), so there are only 8 independent non-hydrogen atoms and 4 hydrogens in the asymmetric part of the unit cell. In addition, compound **1** was found to form single crystals of high diffraction quality. These reasons have determined our choice of the compound for the present EDD analysis.

Experimental Section and Structure Refinement

For an X-ray diffraction study a single-crystal sample with high diffraction quality and all three linear dimensions of ca. 0.3 mm was chosen for data collection at the temperature 120 K with a Siemens P3/PC diffractometer (Mo Kα radiation, graphite monochromator, $\theta/2\theta$ scan method). The total number of the measured reflections was 14 606 ($2\theta_{max} = 94°$, $R_{int} = 0.009$ after averaging of equivalents; an empirical absorption correction was applied). Important data collection conditions, crystal data, and results of the conventional refinement are summarized in Table 1.

The structure was solved and refined with the direct methods and full-matrix least-squares procedures in the anisotropic−isotropic (for hydrogen atoms) approximation using the SHELXTL PLUS program package. An extinction correction was found to be negligible. The atomic coordinates and anisotropic (isotropic for H atoms) displacement parameters corresponding to a conventional refinement are given in the Supporting Information.

Analysis of the anisotropic displacement parameters of the non-hydrogen atoms within the rigid-body LTS model by Schomaker and Trueblood[27] has demonstrated that molecule **1** in crystal may be considered as a rigid body. The agreement between U_{ij} values obtained in the least-squares refinement and those calculated from the LTS model was characterized by the rather low R_U value of 0.018. Libration corrections to the bond lengths did not exceed 0.003 Å. Hirshfeld's "rigid-bond" test[28] was also very satisfactory: the average difference Δ between the atomic mean-squares displacement amplitudes along the interatomic vectors was found to be only 2×10^{-4} Å^2.

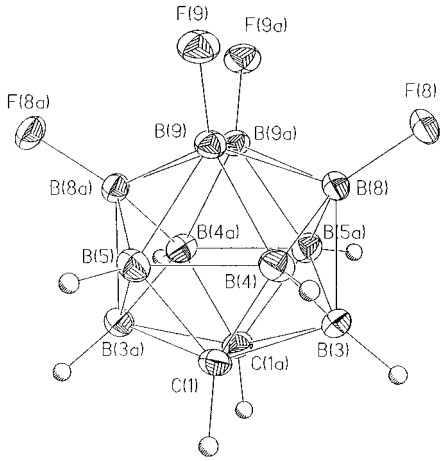

Figure 1. General view of molecule **1** and atom numbering scheme.

Analysis of the EDD in molecule **1** has been performed using the standard dynamic Fourier "*X*−*X*" DED maps and the "static" multipole DED maps calculated with the multipole model and using the XD program package .[24] Results of the last refinement were used for further calculation of the topological characteristics of the electron density.

In the evaluation of the "*X*−*X*" maps a high-order refinement of the diffraction data has been performed in order to obtain a model of the "promolecule". Atomic coordinates and anisotropic displacement parameters for the model of the reference state were refined with 1721 independent high-order reflections having $|F| > 6.0\sigma(F)$ and $\sin\theta/\lambda > 0.65$ Å^{-1}, which resulted in $R = 0.036$, $R_w = 0.033$, and GOF = 0.98. H atom positions in this refinement were fixed together with their isotropic displacement parameters. In the subsequent DED calculations only low-angle data with $\sin\theta/\lambda < 0.75$ Å^{-1} were used in order to decrease the noise on DED maps.

In the multipole refinement the well-known and widely used Hansen and Coppens model of the rigid nonspherical pseudoatom[23] was applied in order to calculate the static DED maps, maps of the Laplacian of the electron density, and the types and positions of the critical points in $\rho(\mathbf{r})$. Multipole expansion for non-hydrogen atoms was taken up to the hexadecapole level ($l = 4$) with no restriction in the local symmetry, and for the hydrogen atoms up to dipole level ($l = 1$) with the cylindric local symmetry. This refinement converged to $R = 0.0265$, $R_w = 0.0229$, GOF = 1.61, and the ratio $N_{ref}/N_{par} = 11.2$.

Results and Discussion

Molecular Structure. The molecular structure of **1** with the atoms presentated as thermal probability ($p = 50\%$) ellipsoids and the atomic numbering scheme are shown in Figure 1. In the crystal, the molecules occupy a special position with the 2-fold axis passing through the middles of the B(9)−B(9a) and opposite C(1)−C(1a) bonds.

All bond lengths and bond angles (Table 2) in the structure studied have expected values typical for the *o*-carborane derivatives studied before. The C−C and B−C bond lengths are equal to 1.632(1) and 1.688−1.719(1) Å. The B−B bond lengths vary in a slightly larger interval (1.775−1.814(1) Å), and the longest B−B bonds correspond to the B(8,9) atoms bonded with the fluorine ones. It is noteworthy that the opposite trend is usually observed in the other studied *o*-carboranes, where the more elongated B−B bonds in the icosahedron cage are closer to the C−C edge,[29] probably because of the higher electrononegativity of the carbons. The stronger electron-

(26) Lebedev, V. N.; Balagurova, E. V.; Polyakov, A. V.; Yanovsky, A. I.; Struchkov, Yu. T.; Zakharkin, L. I. *J. Organomet. Chem.* **1990**, *385*, 307.
(27) Schomaker, V.; Trueblood, K. N. *Acta Crystallogr., Ser. B.* **1968**, *24*, 63.
(28) Hirshfeld, F. L. *Acta Crystallogr., Ser. A.* **1976**, *32*, 239−244.

Table 2. Bond Lengths (Å) and Bond Angles (deg) in the Structure of **1**

F(8)−B(8)	1.364(1)	F(9)−B(9)	1.365(1)
C(1)−B(3)	1.713(1)	C(1)−B(4)	1.686(1)
C(1)−B(5)	1.688(1)	C(1)−H(1)	0.902(9)
C(1)−C(1A)	1.632(1)	C(1)−B(3A)	1.719(1)
B(3)−B(4)	1.780(1)	B(3)−B(8)	1.775(1)
B(3)−H(3)	1.039(9)	B(3)−C(1A)	1.719(1)
B(3)−B(5A)	1.778(1)	B(4)−B(5)	1.785(1)
B(4)−B(8)	1.792(1)	B(4)−B(9)	1.786(1)
B(4)−H(4)	1.105(11)	B(5)−B(9)	1.784(1)
B(5)−H(5)	1.097(10)	B(5)−B(3A)	1.778(1)
B(5)−B(8A)	1.788(1)	B(8)−B(9)	1.806(1)
B(8)−B(5A)	1.788(1)	B(8)−B(9A)	1.811(1)
B(9)−B(8A)	1.811(1)	B(9)−B(9A)	1.814(1)
B(3)−C(1)−B(4)	63.2(1)	B(3)−C(1)−B(5)	116.3(1)
B(4)−C(1)−B(5)	63.9(1)	B(3)−C(1)−H(1)	115.1(5)
B(4)−C(1)−H(1)	122.4(5)	B(5)−C(1)−H(1)	122.0(5)
B(3)−C(1)−C(1A)	61.8(1)	B(4)−C(1)−C(1A)	112.0(1)
B(5)−C(1)−C(1A)	111.5(1)	H(1)−C(1)−C(1A)	115.2(5)
B(3)−C(1)−B(3A)	115.8(1)	B(4)−C(1)−B(3A)	116.3(1)
B(5)−C(1)−B(3A)	62.9(1)	H(1)−C(1)−B(3A)	114.2(5)
C(1A)−C(1)−B(3A)	61.4(1)	C(1)−B(3)−B(4)	57.7(1)
C(1)−B(3)−B(8)	104.0(1)	B(4)−B(3)−B(8)	60.5(1)
C(1)−B(3)−H(3)	120.1(5)	B(4)−B(3)−H(3)	125.3(5)
B(8)−B(3)−H(3)	130.0(5)	C(1)−B(3)−C(1A)	56.8(1)
B(4)−B(3)−C(1A)	103.6(1)	B(8)−B(3)−C(1A)	104.0(1)
H(3)−B(3)−C(1A)	118.8(5)	C(1)−B(3)−B(5A)	103.6(1)
B(4)−B(3)−B(5A)	108.2(1)	B(8)−B(3)−B(5A)	60.4(1)
H(3)−B(3)−B(5A)	122.8(5)	C(1A)−B(3)−B(5A)	57.7(1)
C(1)−B(4)−B(3)	59.1(1)	C(1)−B(4)−B(5)	58.1(1)
B(3)−B(4)−B(5)	108.2(1)	C(1)−B(4)−B(8)	104.4(1)
B(3)−B(4)−B(8)	59.6(1)	B(5)−B(4)−B(8)	108.3(1)
C(1)−B(4)−B(9)	104.2(1)	B(3)−B(4)−B(9)	108.3(1)
B(5)−B(4)−B(9)	60.0(1)	B(8)−B(4)−B(9)	60.6(1)
C(1)−B(4)−H(4)	115.1(6)	B(3)−B(4)−H(4)	117.2(5)
B(5)−B(4)−H(4)	118.2(6)	B(8)−B(4)−H(4)	129.8(6)
B(9)−B(4)−H(4)	130.4(5)	C(1)−B(5)−B(4)	58.0(1)
C(1)−B(5)−B(9)	104.2(1)	B(4)−B(5)−B(9)	60.0(1)
C(1)−B(5)−H(5)	119.5(5)	B(4)−B(5)−H(5)	120.3(4)
B(9)−B(5)−H(5)	127.3(5)	C(1)−B(5)−B(3A)	59.4(1)
B(4)−B(5)−B(3A)	108.6(1)	B(9)−B(5)−B(3A)	108.7(1)
H(5)−B(5)−B(3A)	118.1(4)	C(1)−B(5)−B(8A)	104.8(1)
B(4)−B(5)−B(8A)	108.8(1)	B(9)−B(5)−B(8A)	60.9(1)
H(5)−B(5)−B(8A)	125.8(4)	B(3A)−B(5)−B(8A)	59.7(1)
F(8)−B(8)−B(3)	123.1(1)	F(8)−B(8)−B(4)	122.8(1)
B(3)−B(8)−B(4)	59.9(1)	F(8)−B(8)−B(9)	121.0(1)
B(3)−B(8)−B(9)	107.7(1)	B(4)−B(8)−B(9)	59.5(1)
F(8)−B(8)−B(5A)	122.4(1)	B(3)−B(8)−B(5A)	59.9(1)
B(4)−B(8)−B(5A)	107.3(1)	B(9)−B(8)−B(5A)	107.4(1)
F(8)−B(8)−B(9A)	120.8(1)	B(3)−B(8)−B(9A)	107.6(1)
B(4)−B(8)−B(9A)	107.5(1)	B(9)−B(8)−B(9A)	60.2(1)
B(5A)−B(8)−B(9A)	59.4(1)	F(9)−B(9)−B(4)	121.9(1)
F(9)−B(9)−B(5)	122.4(1)	B(4)−B(9)−B(5)	60.0(1)
F(9)−B(9)−B(8)	121.4(1)	B(4)−B(9)−B(8)	59.9(1)
B(5)−B(9)−B(8)	107.7(1)	F(9)−B(9)−B(8A)	122.0(1)
B(4)−B(9)−B(8A)	107.8(1)	B(5)−B(9)−B(8A)	59.6(1)
B(8)−B(9)−B(8A)	108.0(1)	F(9)−B(9)−B(9A)	121.8(1)
B(4)−B(9)−B(9A)	107.6(1)	B(5)−B(9)−B(9A)	107.2(1)
B(8)−B(9)−B(9A)	60.0(1)	B(8A)−B(9)−B(9A)	59.8(1)

withdrawing effect of the F atoms in comparison with that of carbons in molecule **1** reverses this geometric feature.

Among the other noteworthy geometric characteristics of the molecule **1** we observe that all F−B−B bond angles (120.8−123.1(1)°) are close to the ideal value 121.7° for *exo*-polyhedral angles in the icosahedron,[29] while H−B−B angles split in two different groups, namely H−B−B(8,9,8a,9a) with the values of angles in the interval 126−130°, and other H−B−B (as well as H−B−C and H−C−B) angles varying in the interval 115−125°, which are closer to the normal values in the icosahedron. This result may be caused by repulsion of H(4,5) atoms, and, to a lesser extent, of the H(3) atom, from the neighboring fluorines.

Analysis of the crystal packing shows that molecules in crystal structure of **1** are linked by the intermolecular contacts H(1)···F(8′) ($^1/_2 + X$, $^1/_2 + Y$, $^1/_2 - Z$) and H(1a)···F(9″) ($^1/_2 - X$, $^1/_2 + Y$, $+ Z$) with the corresponding H···F distances and C−H···F angles 2.63 and 2.56 Å and 129.8 and 128.2°, respectively. The icosahedrons in crystal form pseudohexagonal layers parallel to the *XOY* crystallographic plane (Figure 2).

Analysis of the Deformation Electron Density. A conventional method for visualization the charge density redistribution due to formation of the chemical bonds in a molecular system is the deformation electron density mapping. These maps show migration of the electron density with respect to a specially defined reference state ("promolecule")—the hypothetical superposition of the spherically averaged atomic densities. This approach was found to be very useful in the qualitative analysis of the chemical bonding in many cases. Nevertheless it is known that DED maps are often characterized by a deficit of positive maxima in the bonds (sometimes DED values in centers of covalent bonds are even negative, for example, in hydrogen peroxide[30]) due to oversupply of the electron density in promolecule.[12−14] Taking into account the electron-deficient nature of the B−B and B−C bonds in *closo*-carboranes (we should note that the number of valence electrons per chemical bond in such molecules is equal ≈0.45) as well as the delocalization of $\rho(\mathbf{r})$ over the cage and the presence of the four electron-withdrawing F atoms, it is reasonable to assume that DED maxima in molecule **1** might be significantly weakened.

The $X-X$ section of DED passing through atoms B(3), B(8),B(3a), B(8a), F(8), and F(8a) that are coplanar within 0.023 Å and the 2-fold crystal axis (middles of the C(1)−C(1a) and B(9)−B(9a) bonds) is presented in Figure 3a. A perpendicular section through atoms C(1), C(1a), B(9), B(9a), F(9), and F(9a) is given in Figure 3b. Both sections cut the center of icosahedron cage. As might be seen from these figures, the center of the cage is electronically empty (very similar results were obtained in refs 20 and 21) and the positive DED is distributed in the surface layer of the icosahedron. In Figure 3a there are positive DED maxima (0.16 e/Å^3) in the B(3)−B(8) and B(3a)−B(8a) bonds and extended areas of positive DED in B(3)−X−B(3a) and B(8)−Y−B(8a) regions, where X and Y correspond to centers of C(1)−C(1a) and B(9)−B(9a) bonds. Weak minima of DED (−0.12 e/Å^3) are observed inside the cage and near B(8) and B(8a) atoms, which may be due to the electron-withdrawing effect of fluorine atoms. This effect may also cause small shifts of the DED maxima from the B(8)B(9)B(9a) and B(8a)B(9)B(9a) triangle faces above their planes and closer to fluorines. In Figure 3b there are rather small maxima in C(1)−C(1a) and B(9)−B(9a) bonds as well as accumulation of positive DED in centers of triangle faces of the icosahedron.

In general, however, peak heights are rather weak (from −0.15 to +0.20 e/Å^3), and this is in accord with our expectation. Therefore all other following DED sections represent the static multipole maps, where corresponding maxima are higher because of absence the thermal smearing effect on the electron density. For comparison, Figure 4 represents the same section as in Figure 3b for the static multipole DED. We may note

(29) Mastryukov, V. S.; Dorofeeva, O. V.; Vilkov, L. V. *Usp. Khim.* **1980**, *49*, 2377.

(30) Savariault, J. M.; Lehman, M. S. *J. Am. Chem. Soc.* **1980**, *102*, 1298−1303.

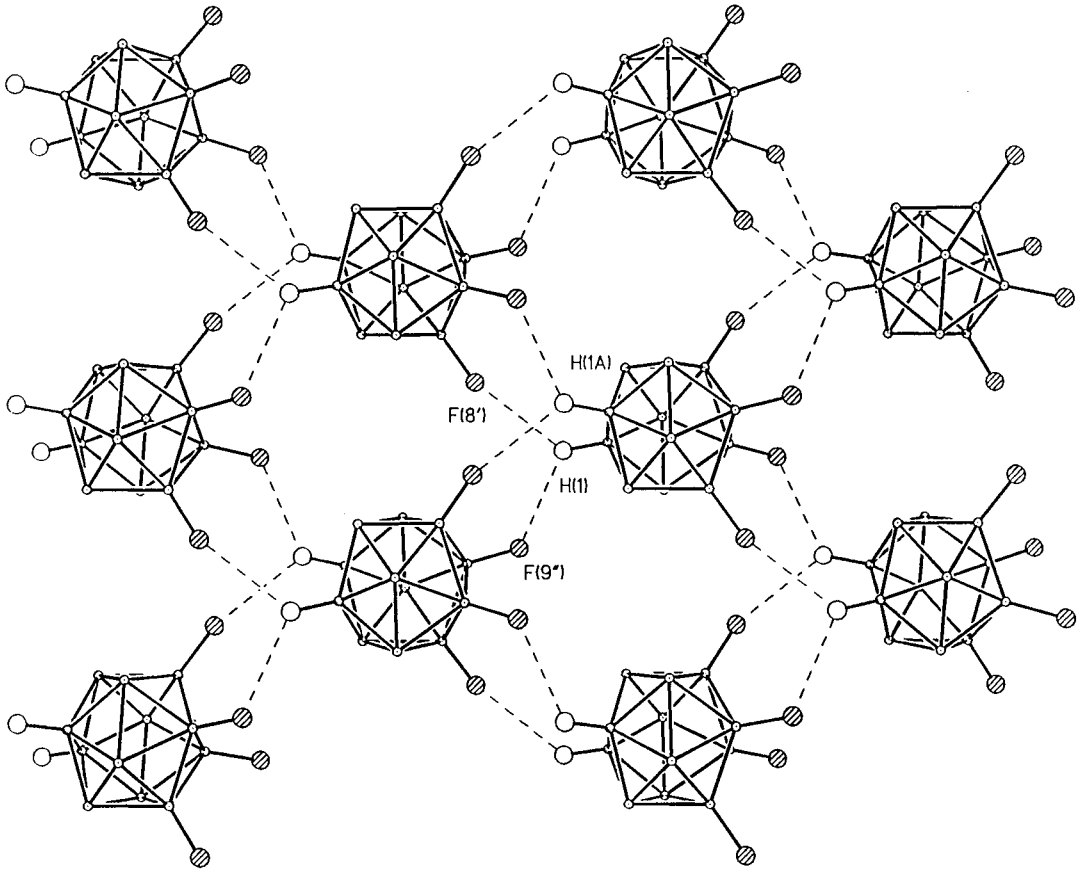

Figure 2. Fragment of crystal structure of **1** in the projection on the *XOY* plane. Possible C−H···F interactions are shown.

that all important features in these maps are similar, but in the static maps they are more pronounced.

Static DED maps in some triangle faces of the icosahedron are presented in Figure 5. In all sections electron density was found to be delocalized over the rings, the maximum DED value being 0.25 e/Å^3. It should be noted that in the C(1)B(4)B(5) plane (Figure 5c) the single DED maximum is shifted to the more electronegative carbon atom. On the contrary, two other sections in the B−B−B planes (Figure 5a,b) are more uniform. The C(1)C(1a)B(3) section (Figure 5d) is characterized by the shift of DED maxima in B−C bonds to carbon atoms and rather weak area of the positive DED in C(1)−(C1a) bond. A small positive DED value in this bond is also seen in Figure 4.

It is interesting to analyze DED features in some five-membered rings of the icosahedron. Corresponding maps in planes B(4a)B(8a)B(9)B(8)B(5a) and C(1)C(1a)B(5a)B(8)B(4) are presented in Figure 6a,b. General features of these maps are very similar with those for some aromatic rings with strong electron delocalization, but there are some noticeable differences. Thus, positive DED areas in the B(H)−B(F) and in particular the B(F)−B(F) bonds are characterized by the double maxima that may reflect the presence of neighboring fluorine atoms. In Figure 6a DED is shifted in the direction to boron atoms bonded with F, and therefore in the opposite B(4a)−B(5a) bond corresponding DED value is small. In Figure 6b the C−B bonds have maxima shifted to carbons (the same was found in the triangle CB_2-face in Figure 5c), and in the C(1)−C(1a) bond the positive DED in this section is also very small. These two maps probably reflect an influence of the adjacent and more electronegative (than boron) fluorine and carbon atoms.

All presented maps demonstrate an essential delocalization of the electron density in the surface layer of the icosahedron and its depletion in the center of the cage. Some polarization of the DED maxima on the surface of icosahedron may be result of the higher electronegativity of fluorine and carbon atoms in comparison with that of boron; however, an influence of these atoms may be different because of their different position in the cage. Nevertheless, analysis of these maps probably cannot give more than simple qualitative information about bonding pattern in the molecule studied. Therefore in this paper we performed a topological analysis of the EDD in **1** based on Bader's "atoms in molecules" (AIM) approach.[10]

Topological Analysis of the Electron Density Distribution. Topological analysis of the EDD in a molecular system based on AIM theory allows one not only to specify a molecular structure in terms of the molecular graph and corresponding bond paths (lines of the highest electron density between the bonded atoms), but also provides an adequate description of the atomic interactions in terms of the charge density characteristics in the so-called critical points of $\rho(\mathbf{r})$.[10] These characteristics usually include the type of critical points, absolute values of $\rho(\mathbf{r})$ and its Laplacian $\nabla^2\rho(\mathbf{r})$ at critical points, bond ellipticities, bond orders, and bond bending characteristics. It is important that such analysis provides not only qualitative but also quantitative information about chemical bonds that is very useful for their comparison in series of similar compounds.

Bond critical points of the (3,−1) type, which are necessary criteria of the covalent chemical bond, were found at all edges of the icosahedron and also in the B−H and B−F bonds of the molecule studied. Important topological characteristics of the electron density in these critical points are summarized in Table 3.

According to theoretical analysis of the topology of $\rho(\mathbf{r})$ by Bader and Legare[17] for the series of borane dianions $B_nH_n^{2-}$ (*n*

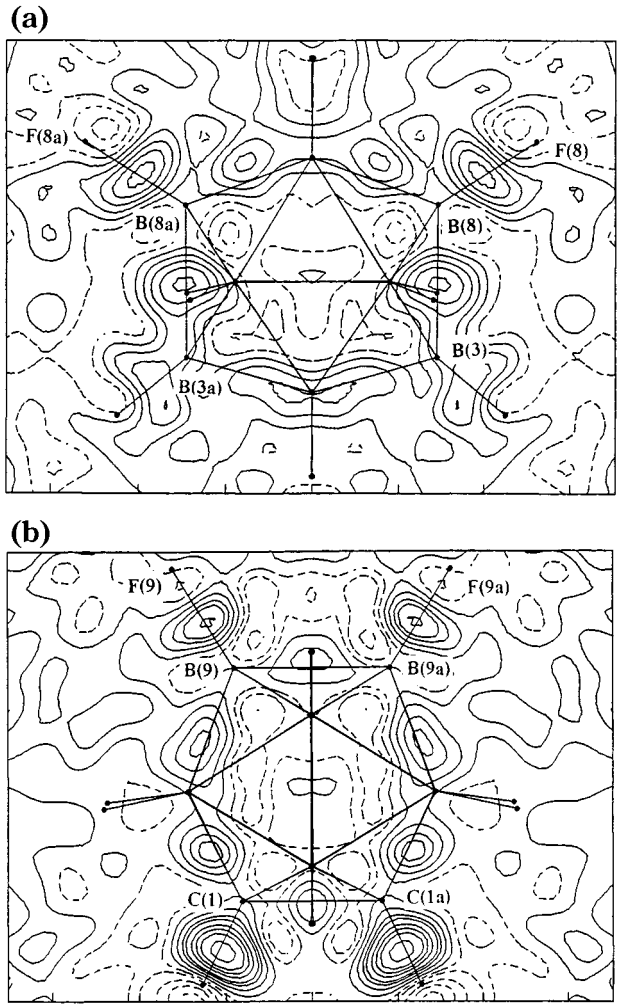

Figure 3. Deformation electron density maps through the center of icosahedron of **1**: (a) in the plane of B(3), B(8), B(3a), B(8a), F(8), F(8a) atoms; (b) in the perpendicular plane of C(1), C(1a), B(9), B(9a), F(9), F(9a) atoms. Interval between isolines 0.04 e/Å^3, negative contours dashed.

= 6, 7, 12) and *closo*-carborane $C_2B_4H_6$ (**2**), electron density in these molecules is strongly delocalized. With increase of the cage volume in deltahedrons the magnitude of $\rho(\mathbf{r})$ at the B−B bond critical points (3,−1) slightly decreases from 0.844 e/Å^3 in $B_6H_6^{2-}$ to 0.797 e/Å^3 in $B_{12}H_{12}^{2-}$. On the other hand, the corresponding value of $\rho(\mathbf{r})$ in carborane **2** increases slightly to 0.876 e/Å^3 in comparison with the isoelectronic dianion $B_6H_6^{2-}$. So, substitution the boron atom in polyhedron by the carbon leads to a small increase of $\rho(\mathbf{r})$ at the B−B bond critical points.

Analysis of the experimental $\rho(\mathbf{r})$ values in (3,−1) bond critical points in the structure of **1** shows that the electron density is delocalized over the icosahedron cage and varies in the interval 0.71−1.16 e/Å^3 (Table 3), having a minimum at the B(4)−B(5) bond and attaining a maximum at the C(1)−C(1a) bond. Estimated standard deviations for $\rho(\mathbf{r})$ values and its Laplacian at the bond critical points were found to be 0.02 e/Å^3 and 0.04 e/Å^5, respectively. We should note, that the values of $\rho(\mathbf{r})$ do not correspond the trends in DED maps, where corresponding maximum at the C(1)−C(1a) bond is very weak. This result reflects the well-known inadequacy in the interpretation of the difference DED maps in deltahedron structures with the strong electron delocalization.

The $\rho(\mathbf{r})$ values at the B−B bonds in the icosahedron cage of **1** vary in the interval 0.71−0.88 e/Å^3. For comparison, the same value in the isoelectronic dianion $B_{12}H_{12}^{2-}$ (**3**) is equal to 0.797 e/Å^3. On the contrary, $\rho(\mathbf{r})$ at the B−C bonds (0.84−0.91 e/Å^3) in **1** is smaller than in carborane **2**. This redistribution is caused probably not only by the increasing of the cage size, but by the electron-withdrawing effect of the fluorine atoms as well. Thus, the mean multipole atomic charges of the F atoms were found to be −0.21e, while those mean value for the adjacent B(8) and B(9) atoms is equal to +0.23e. Other boron atoms have charges in the interval −0.17 to −0.24e, and the charges of carbons is equal to −0.21e. This charge distribution results in the relatively large dipole moment of the molecule **1** equal to 8.2 D, which is close to the experimental value 7.5 D measured in solution.

As was noted earlier, the C(1)−C(1a) bond in the cage of **1** has the largest $\rho(\mathbf{r})$ value at the bond critical point. Theoretical data for similar values in C−C bonds for *o*-carboranes are absent in the literature; however, we may note for comparison that in ethane (see ref 12) the magnitude of $\rho(\mathbf{r})$ in the C−C bond critical point is equal to 1.69 e/Å^3, which is much higher than that in **1**.

Ring critical points (3,+1) were found in all three-membered faces of the icosahedron. The magnitude of $\rho(\mathbf{r})$ in rings was found to be slightly different for BBB, BBC, and CCB faces and varies in the interval 0.70−0.80 e/Å^3. These values are close to those for reference molecules **2** and **3**. It is important to mention that electron density at the bond (3,−1) and ring (3,+1) critical points has quite comparable values, so stabilization of the electron-deficient system in **1** is achieved not only by the accumulation of an excess of $\rho(\mathbf{r})$ along the bond paths but also by the delocalization over the rings of bonded atoms.

Central part of the icosahedron is characterized by the presence of (3,+3) cage critical point which corresponds to a local minimum of $\rho(\mathbf{r})$. The magnitude of $\rho(\mathbf{r})$ at this point is equal to 0.17 e/Å^3 and the critical point is slightly shifted toward the carbon atoms (average distance from this point to boron atoms is 1.695 Å, and to carbon atoms, 1.553 Å). According to theoretical calculations,[17] increasing of the polyhedron size in the series of dianions $B_nH_n^{2-}$ (n = 6, 7, 12) results in strong decreases of $\rho(\mathbf{r})$ at the cage critical points (0.433 e/Å^3 for $B_6H_6^{2-}$ and 0.092 e/Å^3 for $B_{12}H_{12}^{2-}$, respectively). At the same time, values of $\rho(\mathbf{r})$ at the ring (3,+1) critical points for this series of are very close (0.783−0.741 e/Å^3). Our data for carborane **1** are generally in line with these calculations.

An important topological characteristic of the chemical bond is its ellipticity ϵ, which is defined as $(\lambda_1/\lambda_2 - 1)$, where λ_1 and λ_2 are perpendicular curvatures of $\rho(\mathbf{r})$ at the bond critical point. A preferred accumulation of the charge density in a given plane containing the bond path, for example π-plane in ethylene or ring plane in cyclopropane, results in nonzero values of the bond ellipticity. For example, for these two molecules ϵ values are equal to 0.45 and 0.49, respectively.[11] In *closo*-boranes and carboranes with strong delocalization of the electron density over the surface of the cages we may expect much higher values of the bond ellipticities. Table 3 shows that in molecule **1** ellipticities of the cage forming bonds are very large (0.82−5.38), whereas those of the terminal (single) C−H, B−H, and B−F bonds are close to zero. The largest ellipticities have B−B bonds, and namely these bonds were found to be bent in a largest extent. As a measure of the bond bending a deviation Δ of the (3,−1) critical point position from the bond straight line was calculated, and these values are included in Table 3. As might be seen, the value of Δ may be as large as 0.20−0.22 Å (for

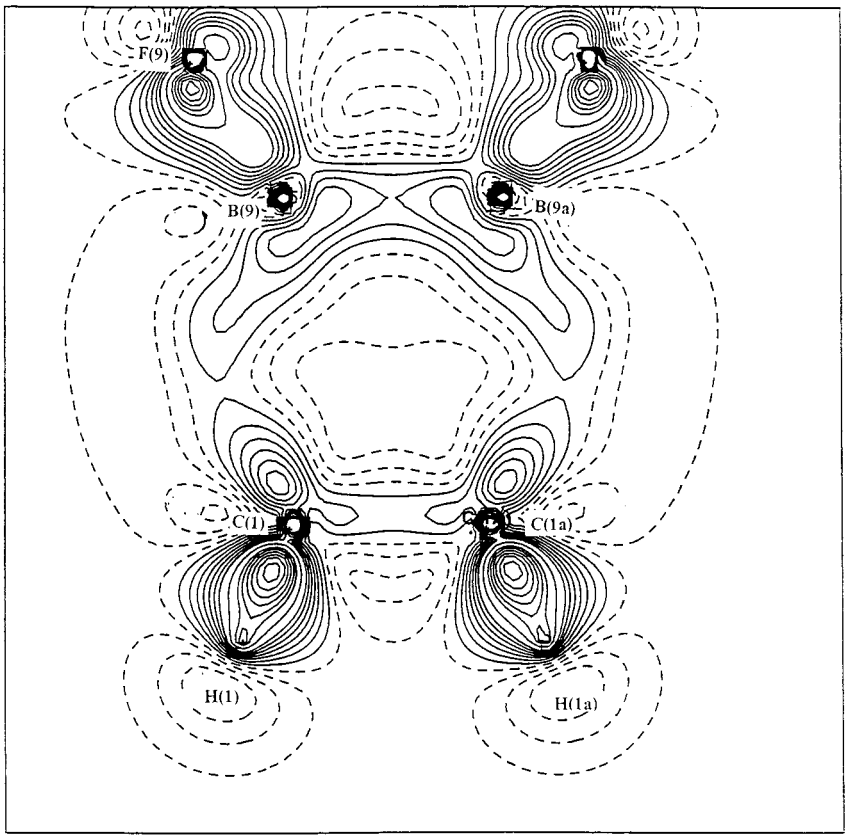

Figure 4. Static multipole deformation electron density in the same plane as in Figure 3b. Interval between isolines 0.05 e/Å^3.

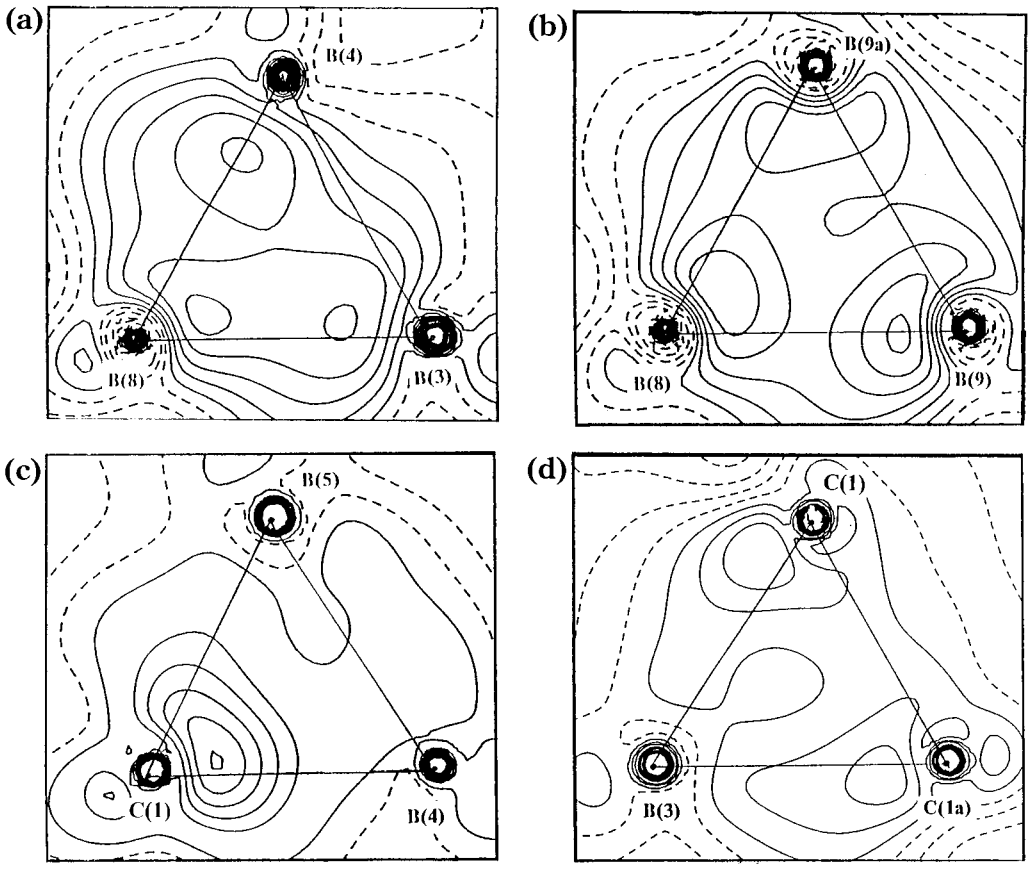

Figure 5. Static multipole deformation electron density in plane of some 3-angle faces of the icosahedron of **1**. Interval between isolines 0.05 e/Å^3.

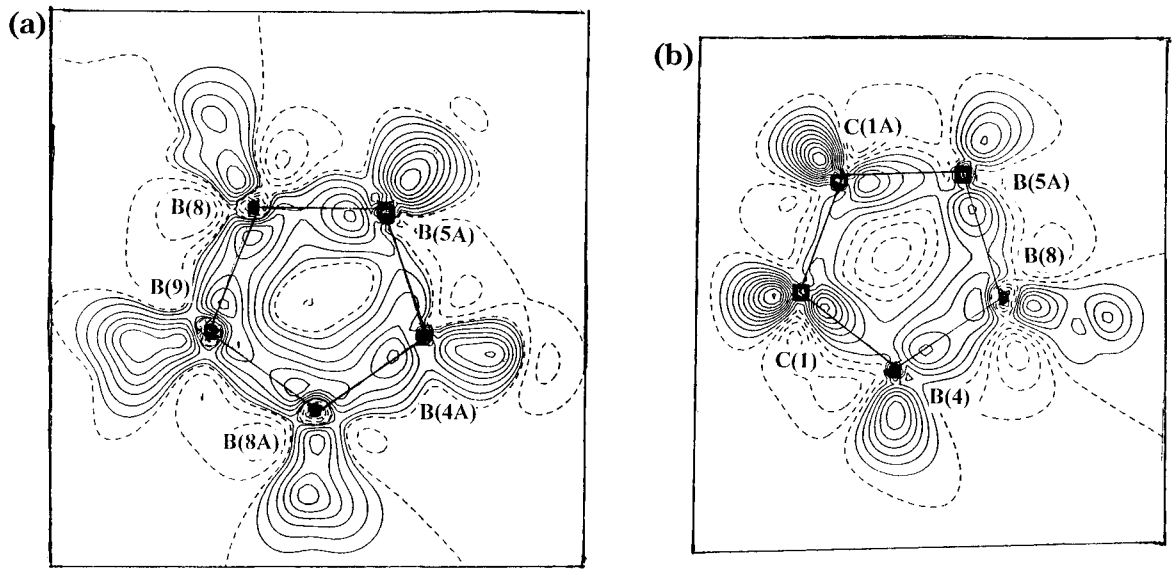

Figure 6. Static deformation electron density in the plane of some 5-membered rings: (a) in the plane of B(4a), B(5a), B(8), B(9), B(8a) atoms; (b) in the plane of C(1), C(1a), B(5a), B(8), B(4) atoms. Interval between isolines 0.05 e/Å^3.

Table 3. Topological Properties of the Electron Density at the (3,−1) Bond Critical Points in the Molecule of **1**[a]

bond	ρ, e Å^{-3}	$\nabla^2\rho$, e Å^{-5}	R_{xr}, Å	R_{bp}, Å	d_1	d_2	Δ	ϵ
C(1)−H(1)	1.86	−18.45	1.06	1.06	0.749	0.311	0.005	0.01
C(1)−B(3)	0.84	−2.00	1.7148	1.726	1.019	0.707	0.097	2.45
C(1)−B(3a)	0.86	−3.93	1.7190	1.723	1.038	0.685	0.062	1.43
C(1)−B(4)	0.886	−2.58	1.6869	1.692	1.093	0.599	0.065	1.72
C(1)−B(5)	0.96	−5.26	1.6866	1.690	1.093	0.597	0.046	1.07
C(1)−C(1a)	1.16	0.54	1.6336	1.633	0.817	0.817	0.050	0.82
B(3)−H(3)	1.32	−14.31	1.20	1.201	0.684	0.517	0.003	0.04
B(3)−B(4)	0.86	−1.24	1.7800	1.834	0.938	0.896	0.222	2.40
B(3)−B(5a)	0.76	−0.37	1.7779	1.826	0.939	0.887	0.205	5.17
B(3)−B(8)	0.88	−2.97	1.7744	1.780	0.900	0.880	0.068	1.64
B(4)−H(4)	1.32	−15.11	1.20	1.20	0.655	0.545	0.006	0.04
B(4)−B(5)	0.71	−0.64	1.7853	1.813	0.938	0.875	0.160	5.35
B(4)−B(8)	0.83	−0.85	1.7930	1.799	0.941	0.858	0.067	3.36
B(4)−B(9)	0.86	−2.79	1.7870	1.802	0.893	0.909	0.115	1.37
B(5)−H(5)	1.30	−15.05	1.20	1.20	0.656	0.544	0.004	0.02
B(5)−B(8a)	0.77	−0.61	1.7874	1.797	0.966	0.831	0.102	5.38
B(5)−B(9)	0.81	−1.98	1.7845	1.802	0.936	0.866	0.123	1.45
B(8)−F(8)	1.40	7.33	1.3637	1.364	0.465	0.899	0.008	0.06
B(8)−B(9)	0.82	−1.27	1.8068	1.813	0.882	0.931	0.070	3.31
B(8)−B(9a)	0.81	−1.64	1.8104	1.814	0.921	0.893	0.050	1.56
B(9)−F(9)	1.45	10.99	1.3640	1.366	0.461	0.905	0.012	0.02
B(9)−B(9a)	0.77	−1.30	1.8135	1.816	0.908	0.908	0.036	3.14

[a] R_{xr}, interatomic (inter-attractors) distance; R_{bp}, bond path; d_1, d_2, distances from the atoms to the bond critical point along the bond path; Δ, deviation of the critical point (3,−1) from the bond straight line (Å); ϵ, bond ellipticity.

the B(3)−B(5a) and B(3)−B(4) bonds). For other B−C and C−C bonds the ellipticities and Δ values are smaller than for B−B bonds, but still they are very large in comparison with the known values for many other nondeltahedral molecules. Theoretical calculation[17] of borane dianions $B_nH_n^{2-}$ also shows very large ellipticities for B−B bonds.

An essential bond bending in the carborane studied results in rather large differences between the bond path (R_{bp}, topological line of the maximum electron density between two bonded atoms) and corresponding interatomic distance (R_{xr}) calculated from the X-ray diffraction data. Some data in Table 3 show that the difference between these two values is as large as 0.05−0.06 Å, which might be a subject of discussion in analysis of the molecular geometry of similar systems. For example, the longest B−B bond lengths in the structure of **1** were found between B(8,9) atoms (see discussion above), but the longest B−B bond path was found for the other B(3)−B(4) and B(3)−B(5a) bonds. Therefore one should be rather careful in discussion of some features of the molecular geometry in carboranes in terms of the convential bond lengths (interatomic distances).

The magnitudes of d_1 and d_2 listed in Table 3 are distances from the atom to the bond critical point along the bond path. These characteristics are rather informative because they are related to the polarity of a bond. Analysis of these values in molecule **1** shows for example, that C−H and B−H bonds have essentially different nature. For C−H bond the critical point is shifted significantly to the hydrogen (according to Bader's theory,[10] a bond critical point should be shifted to the less electronegative atom), while for B−H bonds the difference between d_1 and d_2 values is small. This result reflects an increased acidity of the carbon hydrogens in molecule (**1**) known from its chemical behavior and spectral data. Thus, according to the IR study of different carboranes and their B-substituted derivatives, an increase in the volume of the carborane cage[31] and the presence of electron-accepting substituents at boron

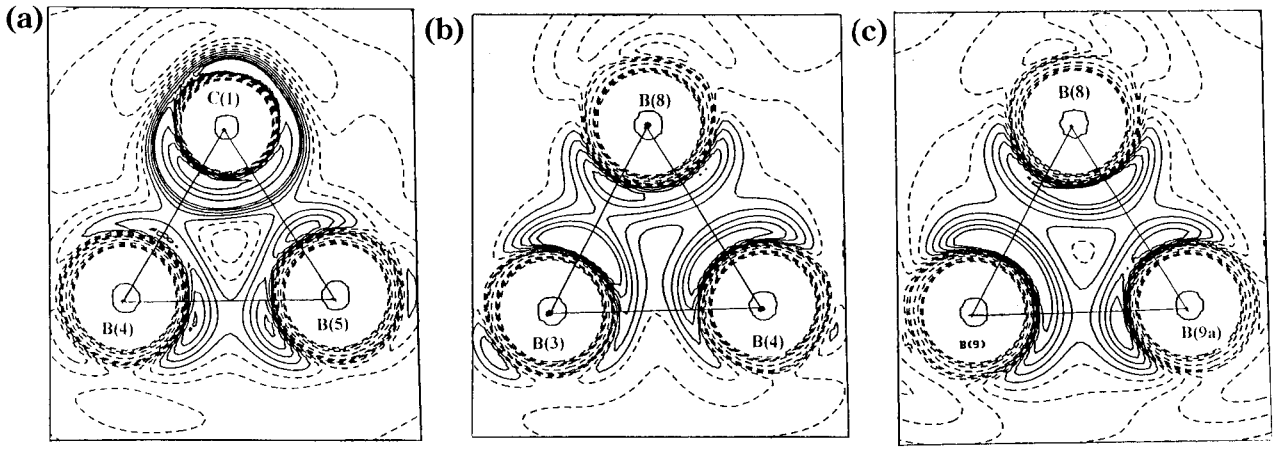

Figure 7. Laplacian of the electron density in the plane of some 3-angle faces of the icosahedron of **1**. Positive contours are dashed, logarithmic scale.

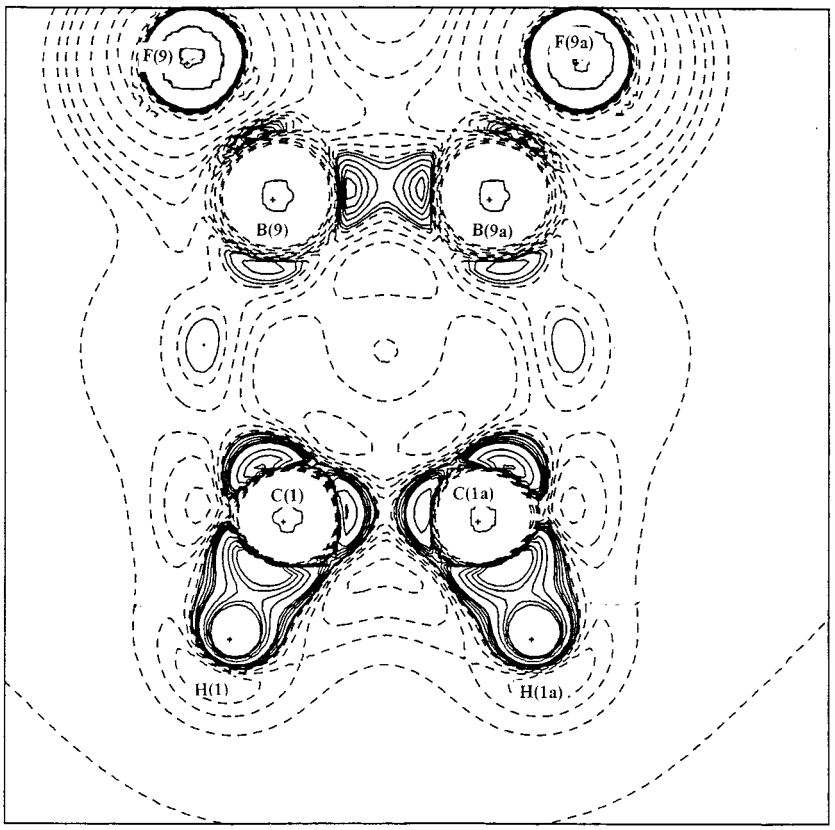

Figure 8. Laplacian of the electron density through the center of the icosahedron of **1** in the same plane as in Figures 3b and 4. Logarithmic scale, positive contours are dashed.

atoms[32] result in an increase of ν(C−H) frequencies that is directly related to the C−H acidity. The more acidic nature of the C−H bonds follows also from formation of the C−H···F intermolecular contacts in the crystal structure of **1** that may be considered as weak hydrogen bonds. As expected, corresponding B−C and B−F bond critical points are shifted to the boron atoms.

Finally, let us discuss the values of Laplacian $\nabla^2\rho(\mathbf{r})$ in the structure of **1**. Laplacian of $\rho(\mathbf{r})$ at the bond critical points contains important information about the nature of bonding and interatomic interactions in a molecular system. In particular, the sign of $\nabla^2\rho(\mathbf{r})$ determines if the electron density is locally depleted in the interatomic region ($\nabla^2\rho(\mathbf{r}) > 0$), or characterized by a local concentration of the electronic charge ($\nabla^2\rho(\mathbf{r}) < 0$). Local concentration of the charge density along the bond path results in negative values of Laplacian in the corresponding regions of the molecular (or crystal) space where the shared (covalent) interactions are dominating. Conversely, the Laplacian is positive for the so-called closed-shell (electrostatic) interactions that are characterized by a contraction of the charge away from the interatomic surface toward each of the nuclei. The domination of closed-shell interactions is a characteristic of highly polar or ionic bonds, weak hydrogen bonds and nonbonded states, such as in He_2.

(31) Leites, L. A.; Vinogradova, L. E. *J. Organomet. Chem.* **1977**, *125*, 37.
(32) Vinogradova, L. E.; Leites, L. A.; Gedimin, V. V.; Kalinin, V. N.; Zakharkin, L. I. *Russ. Chem. Bull.* **1973**, *12*, 2817.

Values of Laplacian of $\rho(\mathbf{r})$ at the (3,−1) bond critical points in molecule **1** are presented in Table 3. All bonds are characterized by the negative sign of this function with only two exceptions for B−F and C(1)−C(1a) bonds where the Laplacian is positive. A positive Laplacian for B−F bonds is quite clear because of their strong polar character, but its small positive value at the C(1)−C(1a) bond is rather unexpected.

The interval of the negative ($-\nabla^2\rho(\mathbf{r})$) values for B−B and B−C bonds in icosahedron is equal to 0.37−2.79 and 1.99−5.25 e/Å^5, and in general these values for B−C bonds are larger. For comparison, Laplacian at the B−B critical point in dianion **3** has similar magnitude and is equal to −3.89 e/Å^5. On the other hand, for B−C bonds in molecule **2** as well as in the electron-precise carboranes $C_2B_3H_5$ (see ref 17) and $C_2B_3(Et)_5$ (experimental charge density study[21]) the Laplacian was found to be slightly positive. This result probably reflects more polar character of B−C bonds in these smaller molecules. Indeed, the (3,−1) bond critical point positions in these two molecules were found to be much closer to the B atoms than in the molecule **1**. In addition, the negative Laplacian for B−C bonds in **1** may be related to the redistribution of the electron density in the icosahedron due to electron-withdrawing effect of the fluorine atoms.

Sections of Laplacian (as maps of the $-\nabla^2\rho(\mathbf{r})$ values) in the three-membered rings C(1)B(4)B(5), B(3)B(4)B(8), and B(8)B(9)B(9a) are presented in Figure 7a−c, respectively. Their comparison with similar multipole static DED maps in Figure 5 shows that Laplacian maps reflect main features of the DED ones, but they are more informative. For most bonds in these sections, negative Laplacian regions corresponding to the concentration of the electron density are shifted from the bond lines, which are related to their large bending and large ellipticity values. Figure 8 represents a Laplacian map through the center of the icosahedron cage in the same section as corresponding DED maps in Figures 3b and 4. The most interesting feature of this map is the positive value of the Laplacian in the homopolar C(1)−C(1a) bond, although its absolute magnitude is not very large (0.54 e/Å^5). On the other hand, however, this bond in the icosahedron frame has the largest value of the total electron density at the bond critical point (1.16 e/Å^3), and this is an essential difference between the positive Laplacian in **1** and other systems with closed-shell interactions such as He_2 or Ar_2.

One possible reason for the unusual Laplacian distribution in the homopolar C−C bond in molecule **1** may be related to the fluorine electron-withdrawing effect. Fluorine atoms pull electron density away from the carborane cage, and in particular this is reflected in a shift of $\rho(\mathbf{r})$ from the more electron-rich C−C bond compared to the B−C ones. Unfortunately, there is no theoretical or experimental data in the literature about electron density distribution for other *o*-carboranes, therefore we cannot compare Laplacian distributions in C−C bonds in **1** with other *o*-carboranes having, for example, donor substituents at the boron atoms. On the other hand, taking into account the well-known ability of *o*-carboranes to isomerize in *m*-carboranes, we may suppose that observed local depletion of the electron density at C−C bond might be a general property of *o*-carboranes. Detailed analysis of the nature of the C−C bond in *o*-carboranes requires an additional investigation.

Acknowledgment. The authors are grateful to the CRDF Foundation (Grant RC2-147) for financial support.

Supporting Information Available: Tables of the X-ray structure determination summary, non-hydrogen atom coordinates and their equivalent displacement parameters, bond lengths, bond angles, anisotropic displacement parameters for non-hydrogen atoms, and hydrogen atom coordinates (6 pages). Ordering information is given on any current mashhead page.

IC9807644